The anti-rebound effect of flexible polymers on impacting drops

M. Smith[*] and V. Bertola[†]
[*] Department of Physics and Astronomy
University of Nottingham
Nottingham NG7 2RD, United Kingdom
[†] Dipartimento di Energetica
Politecnico di Torino
10129 Torino, Italy

Abstract

Very small amount of flexible polymers (of the order of 100 ppm) dissolved into water drops impacting on hydrophobic surfaces are able to completely inhibit drop rebound, which is observed with drops of pure water. This phenomenon, which has been known for about 10 years, is commonly attributed to the stretching of polymer molecules in regions of high velocity gradients, which is believed to cause large energy dissipation in the bulk fluid. In this work we show that this interpretation is not correct, the anti-rebound effect being caused by a dissipative force localized on the contact line.

Introduction

When a droplet of water falls on to a hydrophobic surface, such as the waxy leaf of a plant, the drop is often observed to bounce off [1],[2]. However, for about 10 years it has been known that the addition of very small quantities (~100 ppm) of a flexible polymer such as poly-(ethylene oxide) (PEO) can completely prevent rebound [3], as shown in Figure 1. This is surprising since the shear viscosity and surface tension of such drops are almost identical to those of pure water.

This effect has for some time been explained in terms of the stretching of polymer chains by a velocity gradient in the fluid, resulting in a transient increase in the so-called "extensional viscosity" (the ratio of the first normal stress difference to the rate of elongation of the fluid), which for a polymer solution can be two or three orders of magnitude higher than that of the solvent. In particular, it was suggested that the elongational viscosity causes large energy dissipations during drop spreading immediately after impact on the target surface, so that nothing of the impact kinetic energy is available to propel the drop off the surface itself [3],[4].

This seemed to be confirmed by measurements of the retraction velocity of the liquid after maximum spreading, which for polymer solutions is about one order of magnitude smaller than that measured for the pure solvent [5],[6], and by experimental evidence of a strong correlation between the anti-rebound effect and the fluid elongational viscosity measured with an opposed nozzle rheometer [7].

However, further investigations have demonstrated that in the absence of direct contact between the liquid and the substrate, the anti-rebound effect is no longer observed. A study of drops impacting on small targets [8] suggests that polymer additives do not change the retraction velocity, while independent experiments on Leidenfrost drops (where the liquid is separated from the target surface by a thin vapor layer) [9],[10] show that they cause only a slight reduction of it. Because in these experiments wetting effects are absent or negligible, one must conclude that the retraction velocity reduction observed in drops containing flexible polymers impacting on solid surfaces is due to the drop-surface interaction rather than to an increased energy dissipation connected to the elongational viscosity of the fluid.

Furthermore, measurements of the maximum bouncing height of Leidenfrost drops (indicative of the fraction of the initial kinetic energy which is not dissipated during impact) suggest that in some conditions polymer additives reduce instead of increasing the overall energy dissipation and enhance instead of suppressing bouncing [9],[10]. Therefore, one must conclude that the real cause of this phenomenon is to be sought in the dynamic wetting behaviour of dilute polymer solutions, and not in some bulk property of the fluid such as the elongational viscosity.

This work aims to shed more light on the effect of flexible polymers on the behaviour of impacting drops by means of three independent experiments, which on one hand rule out the bulk viscoelastic properties of the fluid, and on the other hand suggest a more realistic physical mechanism for the anti-rebound effect, based on the polymer molecule dynamics induced by the receding contact line [11].

[†] Visiting Professor, on leave from the University of Edinburgh, UK. E-mail: V.Bertola@ed.ac.uk
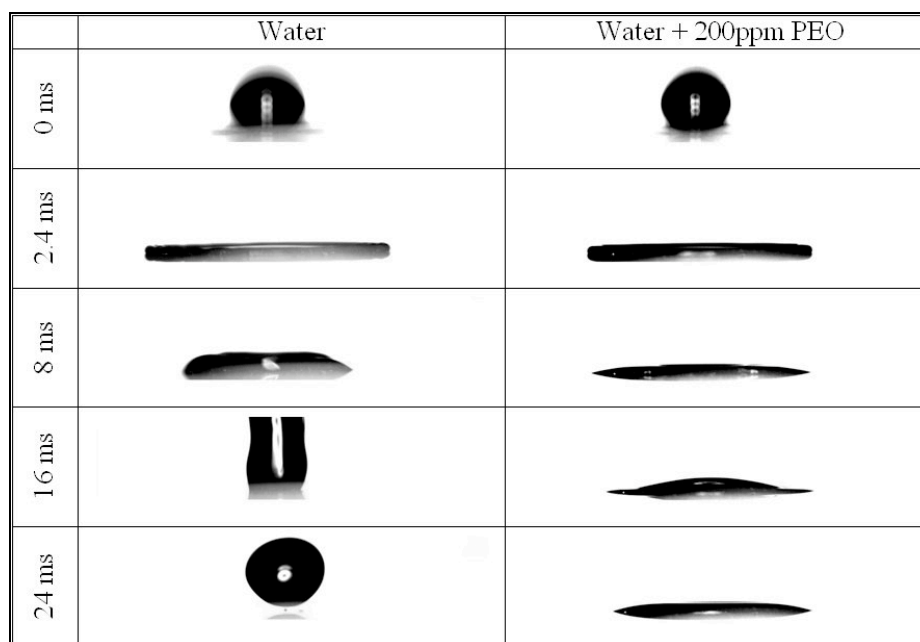
Figure 1. Drop impact on a Fluoropel-coated glass substrate: comparison between de-ionised water and a 200 ppm solution of PEO in the same water.

In the first experiment, the fluid velocity inside the impacting drop is analysed by epifluorescent particle tracking, both during the inertial spreading on the target surface and during the subsequent retraction stage. The comparison between drops of pure water and drops containing a small amount (200 ppm) of PEO shows that the fluid velocity is almost identical, which excludes any elongational viscosity effects in the drop containing the polymer.

In the second experiment, the apparent dynamic contact angle during the retraction stage after maximum spreading is measured for two drops of the same fluids. Whilst the open literature reports several experimental and theoretical studies about the dynamic contact angle of Newtonian drops [12],[13], to the Author's knowledge viscoelastic fluids such as dilute polymer solutions have never been considered so far. Results show that the additive causes a dramatic reduction of the transient contact angle during drop retraction, even if the difference between the final equilibrium values is almost negligible. This suggests that a transient force is exerted on the contact line, opposing its receding movement.

Finally, in the third experiment the behaviour of polymer molecules near the contact line of impacting drops is investigated by direct visualisation of fluorescently stained λ-DNA molecules, which exhibit the same qualitative behaviour of synthetic polymers such as PEO, but are large enough to be visualized by optical microscopy [14]-[16]. It is shown that as the drop edge sweeps the substrate, molecules at the contact line are stretched in a manner similar to other DNA stretching methods such as molecular combing or air blowing techniques [17]. This suggests that the entropic resistance to extension and the hydrodynamic drag of water molecules associated with the polymer chains resist the retraction, slowing the motion of the drop edge.

Materials and Methods

PEO drops were created from a 200 ppm solution in de-ionized water. The PEO, supplied by Aldrich Chemicals in the form of granular powder, had an average molecular weight of 4,000,000 a.m.u. and a typical density of 1210 kg/m^3. The solution was prepared by gently dissolving the polymer into a batch of ultra-pure water, where a large vortex was created by a magnetic stirrer, then mixed for about one hour at low speed. This procedure prevents the formation of non-dissolved polymer clusters, which make the solution inhomogeneous, and at the same time minimizes shear degradation.

The equilibrium surface energy of the polymer solution, measured using a maximum bubble pressure instrument (Krüss PocketDyne), was 69 mJ/m^2, while shear viscosity, measured with a rotational rheometer (Haake MARS II) equipped with a 60 mm plane/plane geometry and Peltier temperature controller, was 1.23 mPa·s.

To probe the details of this edge effect, λ-DNA (148 kbp) stained with YOYO-1 dye at a dye:bp ratio of 1:8 was dissolved in a solution of 200 ppm PEO, at a concentration of 0.2 ppm. The λ-DNA was supplied by New England Biolabs while the YOYO-1 dye was supplied by Invitrogen.

2
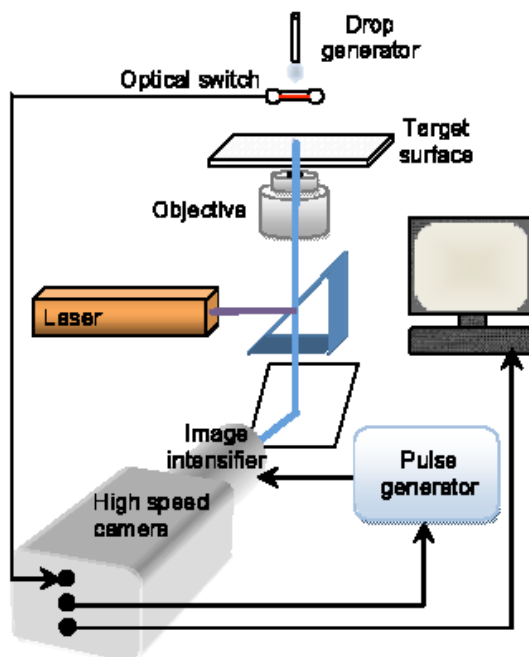
**Figure 2.** Experimental setup for particle tracking and DNA visualisation experiments.

The target surface used in all experiments was a glass slide coated with Fluoropel PFC1302A (Cytonix Corp.), a 2% fluoropolymer solution in low boiling point (135°C) fluorosolvent, with equilibrium contact angles of about 105°. The Fluoropel coating was created by dipping glass slides into the liquid, and then dried at 90°C for 10 minutes to optimize adhesion.

Droplets were formed at the end of a blunt hypodermic needle, suspended from a micrometer adjusted mount, which allowed changing the falling height hence the impact Weber number. The experimental setup used for particle tracking (first experiment) and DNA visualisation (third experiment), shown schematically in Figure 2, was built around an inverted epi-fluorescent microscope containing a x40 objective (NA 0.75) and filter set. Excitation was provided by a pulsed UV laser ($\lambda \sim 355nm$, repetition rate $\sim 8kHz$) for the particle tracking measurements and a visible continuous wave laser ($\lambda \sim 450nm$) for the DNA experiments. The microscope was equipped with a high speed camera (Phantom v9.1) fitted with image intensifier (Lambert Instruments). The falling droplet passed through a light gate triggering collection of a series of images.

For contact angle measurements (second experiment), a 0.838 mm i.d. needle (gauge 18) was placed 185 mm above the target surface. The theoretical free-fall velocity was 1.9 m/s, corresponding to an impact Weber number of about 170 for both water and the polymer solution. Impacts were recorded by a Mikrotron MC1310 camera equipped with a 18–108/2.5 lens (Navitar Zoom 7000) and horizontally aligned with the target surface. Back-to-front illumination was provided by a low-power (2 W) LED backlight (Philips AccentLED) to avoid unwanted heating.

In the first experiment (particle tracking), 2μm fluorescent colloids were diluted with the appropriate solution (de-ionised water or a 200 ppm PEO solution) to a final concentration of <0.001wt%. Drops were released from a height of 100 mm, corresponding to an impact velocity of about 1.4 m/s. Movies for particle velocimetry were collected at 2000 fps ($f_{Laser} \sim 8kHz$) resulting in each colloid being exposed four times in each frame, as shown in Figure 3. During spreading, particles were observed to follow radial paths. A linear fit to each sequence of particles was extrapolated back to the point of intersection with a reasonable error, to estimate the position of the drop centre and corresponding radial distance of each particle. Time was measured relative to the trigger point, and velocity at each radial position (Eulerian approach) was calculated as $V_P = \Delta x\, f_{laser}$.

In the second experiment, images with a resolution of 960×200 pixels were captured at 2500 frames per second. Magnification was kept constant throughout all experiments and lengths on the image could be calculated by comparison with a reference length (typical spatial resolution: 50 pixels/mm). Quantitative data were extracted from images using proprietary software developed in LabView and Matlab environments, which after background subtraction and image optimization measured the base diameter of drops, as well as the left and right contact angles using the drop profile tangent method.
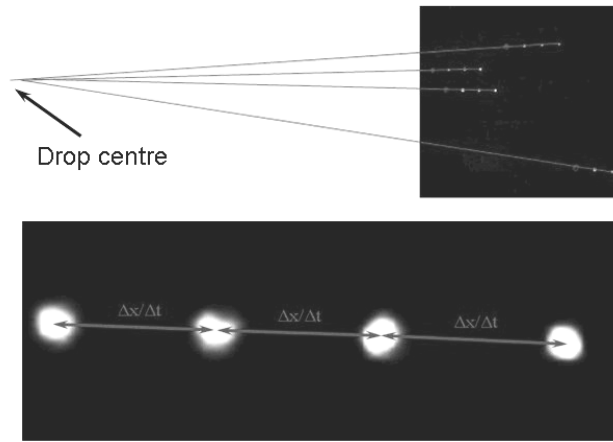
Figure 3. Measurement of the fluid velocity inside the impacting drop by particle tracking


In the third experiment, movies of DNA solutions were collected at a frame rate of 1000 fps with an exposure time of 400μs. λ-DNA is a linear biopolymer which adopts a random coil conformation, with a diameter of about 1.4μm, although its stretched length is about 22 μm [15] and thus visible using a fluorescent microscope (experiments using 10 ppm λ-DNA in water confirmed that DNA, like PEO, is capable of suppressing the rebound of droplets, although at such low concentrations the retraction velocity of the DNA drops is significantly higher). Using a drop height of 20mm and focussing about 2/3 of the way to the maximum spreading radius, the retraction of a droplet was observed.

Results and Discussion
From particle tracking measurements (first experiment), one could obtain the fluid velocity inside the impacting drop at different radial positions during inertial spreading and receding. Figure 4 shows a comparison between the velocities measured inside droplets of pure water (Figure 4a) and 200 ppm PEO solution (Figure 4b). From these plots, one can see that the fluid velocity is almost identical for the two drops, irrespective of the presence of the polymer additive. This is true in particular for the initial retraction velocities of the two drops, which are reported in Figure 5 for different radial positions. When a drop reaches maximum spreading, the elastic energy due to deformation of the surface causes the drop to retract. The speed of the retraction is determined by the amount of stored interfacial energy and the viscosity of the fluid [7]. Consequently, if the two drops, which have similar spreading radii, retract at the same speed, the extensional viscosities must also be similar. For comparison, the retraction velocity of the contact line taken from macroscopic movies is also included. The PEO drop edge, by contrast to the bulk of the fluid, is found to retract an order of magnitude more slowly than that of pure water. Since the current understanding of the phenomenon relies on an increase in the extensional viscosity of the retracting drop, this cannot be a correct picture of the physical mechanism.
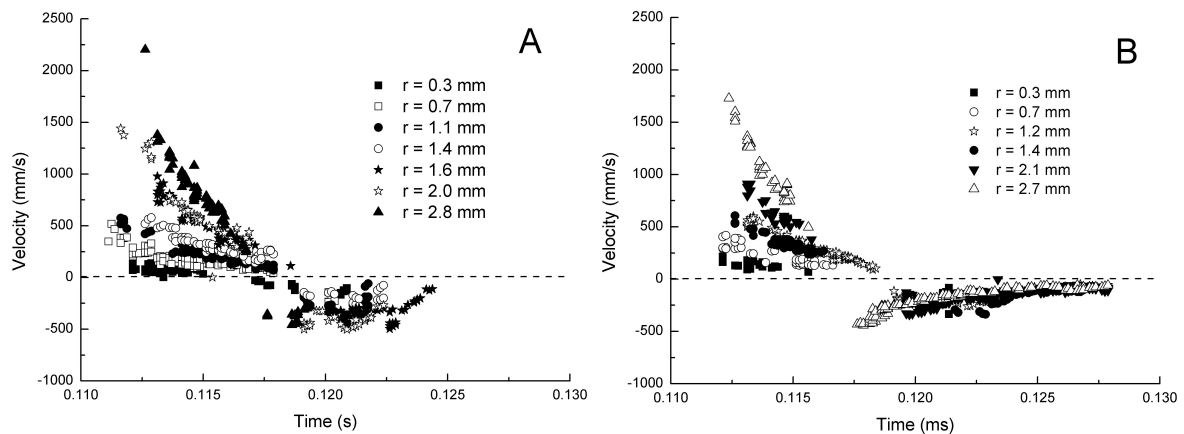

Figure 4. Radial velocity measured in a water drop (a) and in a drop of PEO solution (b), at different distances from the spreading drop centre. Positive values correspond to the expansion stage, negative ones to retraction.
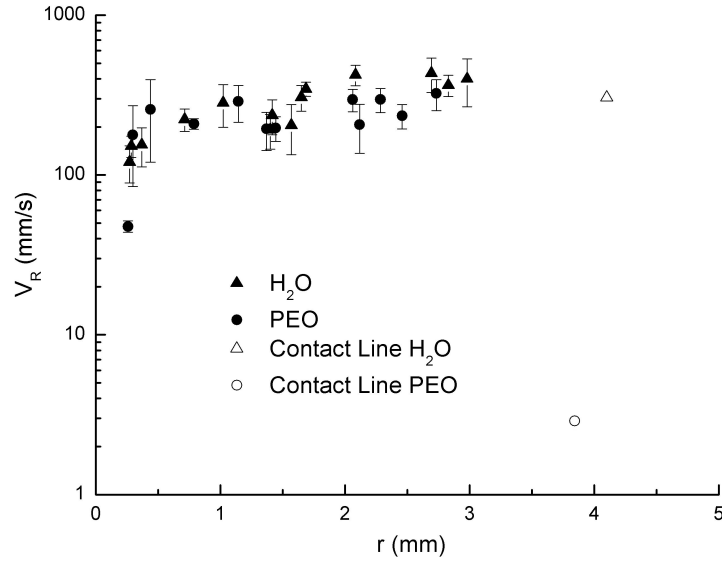
Figure 5. Velocity of the fluid inside impacting drops at the beginning of retraction.

Figure 6 and Figure 7 show, respectively, measurements of the base diameter and of the apparent dynamic contact angles (left and right) obtained in the second experiment from digital images of impacting droplets of the two fluids considered. To allow comparisons, in all these figures the origin of time corresponds to the instant when the drop is at maximum radial spreading, with an apparent contact angle of 90°. If the analysis is limited to base diameter data, one may well conclude that the polymer additive simply causes a reduction of the retraction velocity of the lamella after maximum spreading. However, the retraction velocity measured from pictures corresponds to the contact line velocity, which in the PEO solution drop is one order of magnitude smaller thanthat of the fluid, as shown above.

A closer look at contact angle data (Figure 7) provides a better insight of the phenomenon. Between the end of expansion and the beginning of retraction, the radial velocity is zero (i.e., the apparent contact line does not move) and the contact angle value changes from advancing (> 90°) to receding (< 90°) in a very short time (few milliseconds). Note that such contact angle hysteresis is in principle different from the one usually discussed in the literature, which can be observed when the contact line oscillates about its stable equilibrium position (minimum energy). In this case, the contact angle hysteresis is about an unstable equilibrium position, i.e. about a local surface energy maximum. A naïve interpretation of this phenomenon can be given in terms of the Young-Laplace force balance: the contact angle reduces until the horizontal component of the liquid-vapour interfacial force is large enough to initiate retraction.
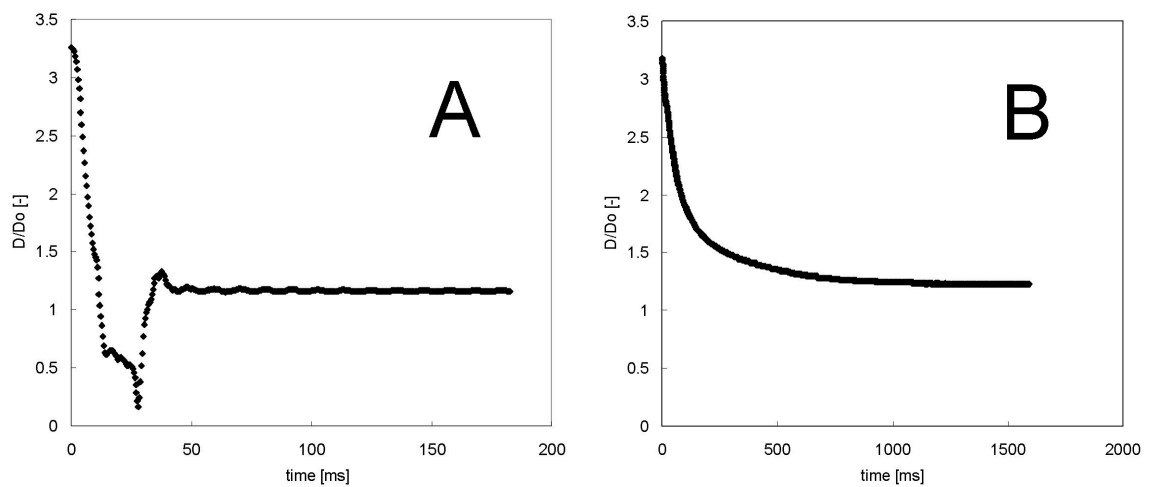
Figure 6. Drop diameter during the retraction stage, normalised with respect to the equilibrium diameter, D_0, for a water drop (a) and one of PEO solution (b).
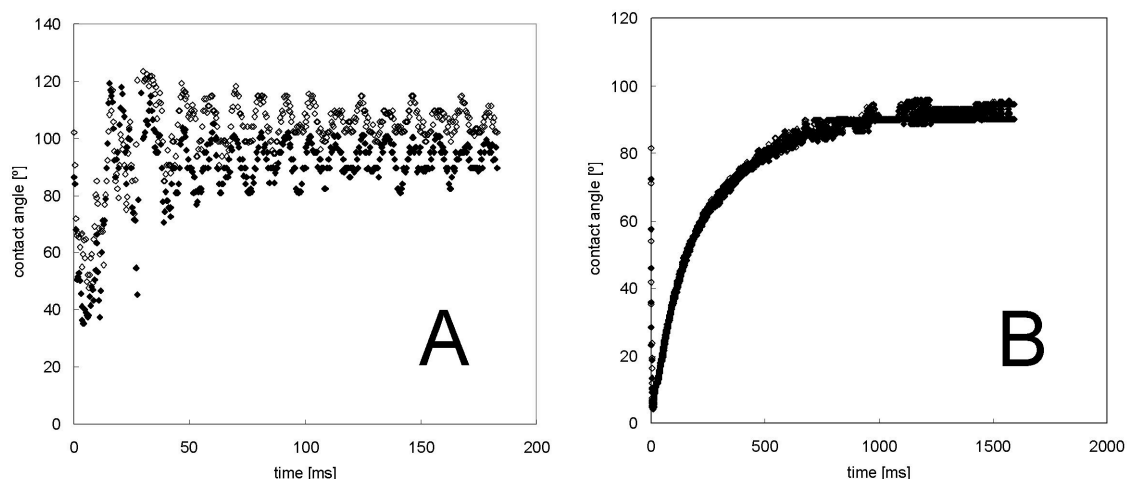
Figure 7. Left (open symbols) and right (filled symbols) apparent contact angles during the retraction stage, for a water drop (a) and one of PEO solution (b).

Strictly speaking, the Young-Laplace equation should not be applicable even if the radial velocity is zero because the system is out of equilibrium, however the timescale of the phenomenon is still much longer than molecular timescales ($\sim 10^{-7} \div 10^{-9}$ s [18],[19]). Contact angle hysteresis around the equilibrium value is generally understood in terms of roughness and/or chemical heterogeneity of the surface [20]. More recently, it has been proposed that it can be caused by a liquid film left behind the contact line during retraction [21]-[23].

While drops of pure water initiate retraction when the contact angle has reached a value around 45°, as shown in Figure 7a, for drops containing the additive retraction begins only when the dynamic contact angle is very small (Figure 7b). This suggests that the horizontal component of the driving force required to initiate the movement of the contact line is much larger than in the case of pure water, as if the contact line was pinned on the surface, or encountered some form of frictional resistance. Moreover, because the advancing contact angle (during drop spreading) is similar for all drops, one can conclude that polymer additives affect dramatically the contact angle hysteresis.

Since both drops of pure water and those of polymer solution impact on identical surfaces, the difference observed in the contact angle hysteresis cannot be interpreted in terms of surface roughness or chemical heterogeneity. Thus, the only options available are: (i) the polymer additive changes the chemical structure of the surface, (ii) it changes the properties of the liquid film left behind the contact line during retraction, (iii) a combination of the two.
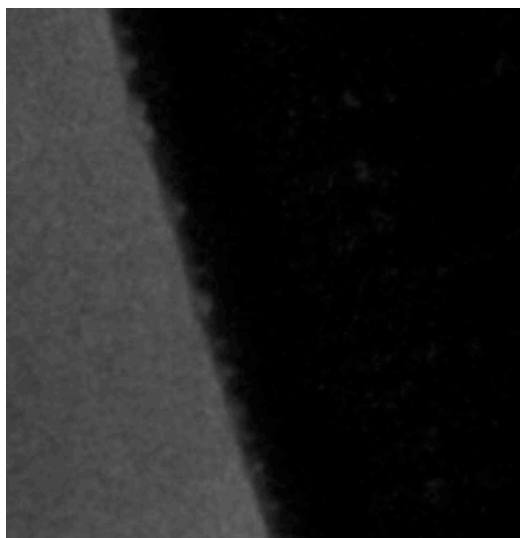
Figure 8. High-magnification (40x) image of the drop edge during retraction.

6
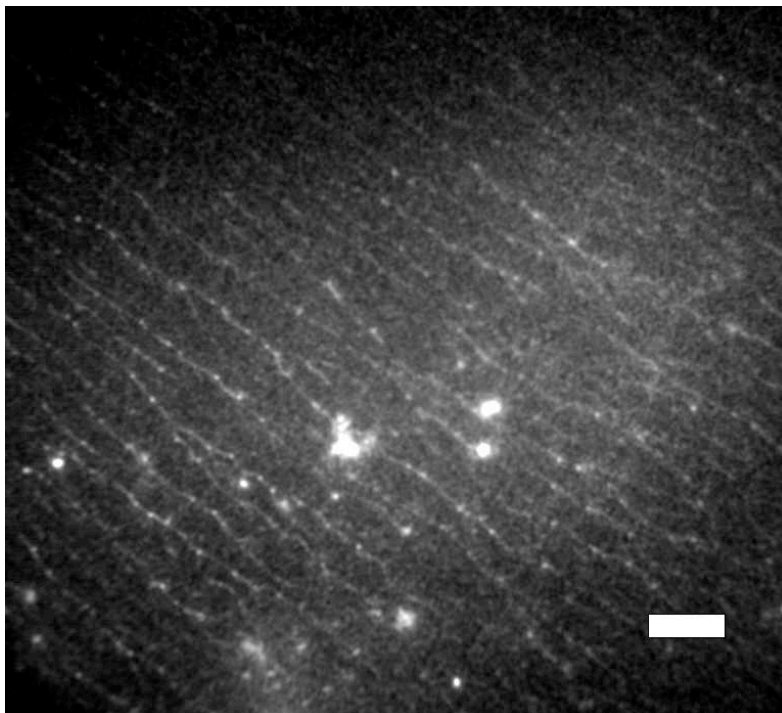
Figure 9. Visualization of stretched DNA molecules left on the impact surface after the transit of the retracting edge of the drop (the scale bar in the bottom-right corner is 20μm).

To further analyse the phenomena occurring in correspondence of the contact line, fluorescent λ-DNA was added to the impacting drop and observed through an optical microscope equipped with image intensifier. A high-magnification detail of the retracting contact line is shown in Figure 8: the drop edge is not smooth, but exhibits several microscopic fingers protruding on the impact surface, in the direction opposite to the contact line movement, exactly as if they were pulled out by an external resisting force. These fingers persist for several frames at a time before disappearing. The fingers fluoresce brightly and are of comparable size to stretched DNA molecules.

After the passing of the contact line, stretched DNA molecules can be observed on the substrate, oriented in the direction perpendicular to the contact line, as shown in Figure 9. This bears strong similarities with other DNA stretching methods, such as molecular combing or air blowing techniques [17]. In particular, in these techniques DNA molecules are stretched using combination of hydrodynamic and surface forces arising when a liquid meniscus moves on a solid surface. For example, in molecular combing such meniscus is created by slowly pulling out a plate from a solution containing DNA. The same conditions occur also when an impacting droplet retracts on the target surface after maximum spreading, the only difference being that this process is orders of magnitude faster than molecular combing, where the typical velocity of the meniscus is 0.2 mm/s.

These results suggest that the contact line retardation observed during the retraction of drops of polymer solutions as compared with drops of the pure solvent is caused by the polymer molecules stretching occurring when the receding contact line sweeps the impact surface. This can be interpreted, from a macroscopic point of view, as an additional, dissipative force acting on the contact line and opposed to its movement, or contact line friction.

Conclusions

The anti-rebound phenomenon, which is observed when small amounts of flexible polymers are dissolved into drops impacting on hydrophobic surfaces, was investigated by means of three different experiments, logically connected to one another, which suggest a physical picture alternative to the current understanding. In the first experiment, PTV measurements of the local fluid velocity inside impacting drops show that there are no significant differences between drops of polymer solution and those of pure solvent. On the contrary, the recoil velocity of the contact line only is one order of magnitude smaller for the polymer solution drop.

These results showed that the bulk properties of the fluid, such as the elongational viscosity, do not have a significant role in preventing drop rebound, and suggested to carry out further investigations focusing on the contact line, which was done in a second experiment. Measurements of the apparent contact angle showed that in drops of PEO solution this quantity is much smaller than in drops of pure water throughout the retraction stage,

although it tends to the same final equilibrium value for long observation times. This means that in order to initiate and maintain the receding movement of the contact line in drops of the polymer solution, the horizontal component of the driving force must be larger than in the case of drops of pure solvent, which suggests the existence of some sort of dissipative force arising on the contact line.

The origin of such force was revealed by the third experiment, where fluorescent DNA molecules were dissolved into an impacting drop of a PEO solution and visualised by optical microscopy. In particular, it was shown that as the drop edge moves on the surface it leaves behind stretched DNA molecules, similar to what happens in some well-known DNA stretching techniques. Thus, one can conclude that the ensemble of transient and local forces exerted by stretching polymer molecules on the contact line causes an overall dissipative force which opposes the contact line movement.

The results of these experiments overturn the current understanding of the anti-rebound effect. While so far it was believed the cause of this phenomenon is one of the bulk properties of the drop (i.e., the elongational viscosity of the polymer solution), in a more realistic picture the anti-rebound effect is caused by an effective contact line friction, due to the coil-stretch transition of polymer molecules dissolved in the drop.

Acknowledgments

References
[1] Rein, M., *Fluid Dyn. Res*. 12: 61-93 (1993).
[2] Yarin, A.L., *Annu. Rev. Fluid Mech.* 38: 159-192 (2006).
[3] Bergeron, V., Bonn, D., Martin, J.Y., and Vovelle, L., *Nature* 405: 772-775 (2000).
[4] Bergeron, V., *C.R. Physique* 4: 211-219 (2003).
[5] Crooks, R. and Boger, D.V., *J. Rheol.* 44: 973-996 (2000).
[6] Bertola, V., *Exp. Fluids*, 37: 653-664 (2004).
[7] Crooks, R., Cooper-White, J., and Boger, D.V., *Chem. Eng. Sci.* 56: 5575-5592 (2001).
[8] Rozhkov, A., Prunet-Foch, B., and Vignes-Adler, M., *Phys. Fluids* 15: 2006-2019 (2003).
[9] Bertola, V., *22nd European Conference on Liquid Atomization and Spray Systems*, Como, Italy, September 2008, Paper ILASS08-13-16.
[10] Bertola, V., *Int. J. Heat Mass Transf.* 52: 1786-1793 (2009).
[11] Smith, M.I., and Bertola, V., *Phys. Rev. Lett.* 104, 153901 (2010).
[12] Bracke, M., Voeght, F.D., and Joos, P., *Prog. Coll. Polym. Sci.* 79: 142-149 (1989).
[13] Roisman, I.V., Opfer, L., Tropea, C., Raessi, M., Mostaghimi, J., and Chandra, S., *Coll. Surf. A: Physicochem. Eng. Aspects* 332: 183-191 (2008).
[14] Morikawa, K., and Yanagida, M., *J. Biochem.* 89: 693-696 (1981).
[15] Smith, D.E., and Chu, S., *Science* 281: 1335-1340 (1998).
[16] Ladoux, B., Quivy, J.-P., Doyle, P.S., Almouzni, G., and Viovy, A.-L., *Science Progress* 84: 267-290 (2001).
[17] Kim, J.H., Shi W., and Larson, R.G., *Langmuir* 23: 755-764 (2007).
[18] Barnes, A.C., Neilson, G.W., and Enderby, J.E., *Journal of molecular liquids* 65-66: 99-106 (1995).
[19] Borodin, O., and Smith, G.D., *Macromolecules* 33: 2273-2283 (2000).
[20] de Gennes, P.-G., *Rev. Mod. Phys.* 57: 827-863 (1985).
[21] Chibowski, E., *Adv. Coll. Interface Sci.* 103: 149-172 (2003).
[22] Chibowski, E., *Adv. Coll. Interface Sci.* 113: 121-131 (2005).
[23] Chibowski, E., *Adv. Coll. Interface Sci.* 133: 51-59 (2007).